Parametric amplification of the signals in the electrostatic graviinertial sensor

Gilavdary I.[1], Mekid S.[2], Riznookaya N.[1]

[1]Belarusian National Technical University,
Nezavisimosty Ave., 65, Minsk 220013, Belarus
[2]King Fahd University of Petroleum & Minerals, Mechanical Engineering Department,
Dhahran 31261, Saudi Arabia

Received 21.02.2017
Accepted for publication 12.04.2017

Abstract

The challenges of designing simple, reliable, and high sensitivity graviinertial sensors are investigated. The sensor comprises a proof mass (PM) and is fixed with the housing by the elastic torsion suspension. PM makes small rotations under the action of gravitational forces or inertial forces.

The distinctive features of the sensor are that the differential electrostatic system provides simultaneous reading of the desired signal and a control the torsional rigidity of suspension. In addition, the PM's rotational angular velocity transforms in the alternating current flowing through the capacitors. The presence of alternating current (AC) voltage sources allows to get the parametric amplification of AC and significantly to improve the sensitivity of the sensor. In the simplest case, the sensor does not contain any feedback circuits.

As an example, calculations of the micromechanical linear accelerations confirm that the periodic modulation of the coefficient of elastic stiffness of the suspension can significantly increase the sensitivity in the low frequency range, even in the absence of parametric resonance.

Conditions for suppressions of background current participating in the output signal from a parametric pumping due to the asymmetry of the differential circuits are set. The frequency characteristics calculations of the sensor were carried out. It is expected, that the proposed sensor design ensures minimum noise level, which can be achievable in the graviinertial sensors. This design and the constructed theory can serve as a basis for creating a wide range of graviinertial devices operating on a movable base, for example, linear and angular accelerometer, gravity gradiometer, gravimeters, and inclinometers, which can be realized in the hybrid and in the micromechanical versions.

Keywords: differential capacitive sensor, modulated stiffness, parametric amplification, gravity gradiometer, linear accelerometer.

DOI: 10.21122/2220-9506-2017-8-2-108-121

Адрес для переписки:
Джилавдари И.З.
Белорусский национальный технический университет,
пр. Независимости, 65, г. Минск 220013, Беларусь
e-mail: gilavdary@mail.ru

Address for correspondence:
Gilavdary I.
Belarusian National Technical University,
Nezavisimosty Ave., 65, Minsk 220013, Belarus
e-mail: gilavdary@mail.ru

Для цитирования:
Gilavdary I., Mekid S., Riznookaya N.
Parametric amplification of the signals in the electrostatic graviinertial sensor.
Приборы и методы измерений.
2017. – Т. 8, № 2. – С. 108–121.
DOI: 10.21122/2220-9506-2017-8-2-108-121

For citation:
Gilavdary I., Mekid S., Riznookaya N.
Parametric amplification of the signals in the electrostatic graviinertial sensor.
Devices and Methods of Measurements.
2017, vol. 8, no. 2, pp. 108–121.
DOI: 10.21122/2220-9506-2017-8-2-108-121

Параметрическое усиление сигналов в электростатическом гравиинерционном датчике

Джилавдари И.З.[1], Мекид С.Н.[2], Ризноокая Н.Н.[1]

[1]Белорусский национальный технический университет,
пр. Независимости, 65, г. Минск 220013, Беларусь
[2]Университет нефти и полезных ископаемых короля Фадха,
Дхахран 31261, Саудовская Аравия

Поступила 21.02.2017
Принята к печати 12.04.2017

Рассматривается задача создания простого, надежного и высокочувствительного маятникового гравиинерционного датчика. Датчик содержит подвижную массу, удерживаемую относительно корпуса с помощью упругого торсионного подвеса. Подвижная масса совершает малые повороты под действием момента силы, обусловленного действием гравитационных сил или силы инерции. Отличительная особенность датчика состоит в том, что дифференциальная электростатическая система обеспечивает одновременное считывание полезного сигнала и уменьшение крутильной жесткости подвеса. Также особенность датчика состоит в том, что его чувствительность определяется угловой скоростью поворота подвижной массы и пропорциональной ей амплитудой переменного тока, протекающего через конденсаторы. Наличие в датчике источников переменного напряжения позволяет осуществлять параметрическое усиление переменного тока и существенно увеличивать его чувствительность. В простейшем варианте в датчике отсутствуют цепи обратных связей.

На примере микромеханического линейного акселерометра путем расчетов доказывается, что периодическая модуляция коэффициента жесткости упругого подвеса позволяет существенно увеличить чувствительность прибора в области низких частот, даже в условиях отсутствия параметрического резонанса. Анализируются условия подавления фоновых составляющих тока, проникающих в выходной сигнал от источников переменного напряжения вследствие несимметричности дифференциальной электрической цепи.

Подобная конструкция и построенная теория могут служить основой при создании широкого круга различных гравиинерционных приборов, работающих на подвижном основании, таких как линейные и угловые акселерометры, гравитационные градиентометры, гравиметры, наклономеры, виброметры, в том числе в гибридном или микро исполнении.

Ключевые слова: дифференциальный емкостной датчик, модулированная жесткость, параметрическое усиление, гравитационный градиентометр, линейный акселерометр.

DOI: 10.21122/2220-9506-2017-8-2-108-121

Адрес для переписки:
Джилавдари И.З.
Белорусский национальный технический университет,
пр. Независимости, 65, г. Минск 220013, Беларусь
e-mail: gilavdary@mail.ru

Address for correspondence:
Gilavdary I.
Belarusian National Technical University,
Nezavisimosty Ave., 65, Minsk 220013, Belarus
e-mail: gilavdary@mail.ru

Для цитирования:
Gilavdary I., Mekid S., Riznookaya N.
Parametric amplification of the signals in the electrostatic graviinertial sensor.
Приборы и методы измерений.
2017. – Т. 8, № 2. – С. 108–121.
DOI: 10.21122/2220-9506-2017-8-2-108-121

For citation:
Gilavdary I., Mekid S., Riznookaya N.
Parametric amplification of the signals in the electrostatic graviinertial sensor.
Devices and Methods of Measurements.
2017, vol. 8, no. 2, pp. 108–121.
DOI: 10.21122/2220-9506-2017-8-2-108-121

Introduction

Due to the rapid development of micro- and nano satellites weighing not more than 100 kg and 10 kg, respectively, [3], which are used for the study of celestial bodies and asteroids from outer near space, as well as for studies surface of these objects, there is an urgent need for the development of simple, low-cost and small-size graviinertial devices for placement in these satellites. The results of these studies can are used to examine the internal structure of the heavy bodies, as well as to detect heterogeneities located close to the surface, for example, that may be required during construction anything objects on them [4–7].

Graviinertial devices include, for example, gravity gradiometers, gravimeters, accelerometers, inclinometers, vibration meters and others. Gravity Gradiometers (GG) used for measurements on moving objects have particular importance among these devices. The development of GG – this is one of the most difficult problems of modern instrumentation design [1, 8]. Currently used GG could be divided into two types [1]: the first type is «warm» devices that operate at room temperature, constructed on the basis of rotating linear accelerometers e.g. devices FTG (Full Tensor Gradiometer) or Air-FTG and the AGG (Airborne Gravity Gradiometer), developed by Lockheed Martin Corporation. GG with nonrotating linear accelerometers can be attributed here also, which were designed by ESA (European Space Agency) and existed for 4 years; 2009 to 2013 within the framework of the program GOCE (Gravity field and steady-state Ocean Circulation Explorer) on board Low Earth Orbit satellite [36–38].

The second type of GG is «cold» devices operating at the boiling temperature of liquid helium, constructed on the basis of angular accelerometers e.g. the devices HD-AGG (High Definition Airborne Gravity Gradiometry) and VK1, developed by GEDEX (Gedex Systems Inc.), University of Western Australia (UWA) and the University of Maryland (UM). The record of low error in «cold» GG which is under development is focused on the achievement of error 1 Eo (Eo – Eötvös, $1Eo = 10^{-9}$ s^{-2}) at the time interval of measurement of one second and noise level of 1 Eo / $Hz^{1/2}$ in the frequency band of 0.001 to 1 Hz [1, 2, 8].

It is recognized that «warm» and «cold» GG have common disadvantages: they are expensive, heavy and bulky, making them difficult to be used in the near space, because they can not be hosted in micro- and nano satellites. Therefore, the creation of simple and small-sized GG and other graviinertial devices is an actual problem of modern instrumentation. It seems obvious that these devices should be carried in a «warm version» to eliminate the need to create the reserves of liquid helium in satellites.

The development of compact GG is primarily linked with the advent of MEMS (micro-electromechanical systems) technology [9, 15, 19]. However, specific problems exist when fabricating graviinertial devices using MEMS method. First problem is that elastic hangers for the proof mass (PM) must satisfy two conflicting requirements: on the one hand, they must have a high flexibility in the direction associated with the axis of sensitivity of the instrument and, on the other hand, they must have a high strength to resist gravitational action and to withstand shocks and vibrations occurring during start and progress in the space orbit [18].

The second problem is the creation of highly sensitive readout signals generated by the movements of elastically suspended PM having small size and low power consumption. Capacitive displacement sensors can respond these requirements [16]. However, the standard capacitive sensors can only be used with additional radio frequency (RF) generators with a frequency of about (10^5–10^6) Hz to trigger them. The main drawback of these sensors is the presence of parasitic capacitances, and, RF signals that can penetrate in the output circuits of the sensors and generate additional noise limiting the sensitivity of the devices [10, 17, 23, 35].

Third problem is the noise generated inside the instrument [20]. It is known, that with decreasing device size, there is an increase in the zero drift and in the ratio noise/signal [10–13]. In particular, the growth of the 1/f noise with a decrease in the size of the conductive elements is known [14]. Presumably, for these reasons in the open press there is no information on the use of GG constructed based on integrated technologies.

One of the possible ways to reduce the noise in the small size GG is to develop a hybrid design in which the PM has size as large as it possible [18] with a possible weight of from 100 to 200 g. For measurements in the near-Earth space, the «hybrid» would have a mass of 1 kg, the volume of 1 dm^3 and 0,001 sensitivity Eo / $Hz^{1/2}$. For this design to provide a measurement time of 1 s, the operating frequency should be below 0.04 Hz and the resonance frequency of 1 Hz [8, 18]. At the same time, for the purpose of

«planetologistik» it is sufficient to have a sensitivity of GG 1 Eo / $Hz^{1/2}$ [15, 19].

The purpose of this paper is to offer a new concept of building a simple and reliable «warm» electrostatic pendulum sensor, which has high sensitivity and low noise. This concept can be used in the development of graviinertial devices capable of operating both on Earth and in space, and facilitate the solution of the above three problems arising in the development of GG.

Features of the proposed graviinertial sensor

Schematic description of the graviinertial sensor (GIS) is illustrated in Figure 1. The sensor comprises a pendulum elastically suspended in electrical field that is generated by the differential capacitive system and the sources of direct and alternating voltage. It is assumed, that the frequency of the AC voltage is higher than the frequency of the signals being measured, but is low enough to electromechanical sensor circuit considered as a circuit with lumped elements. The electric field sensor performs two functions; it reduces the rigidity of the torsional suspension and provides a readout of the desired signal. The first of these features facilitates the solution to the first problem mentioned previously, since the electric field decreases the known resonant frequency of the sensor. The less the resonant frequency of the sensor, the more sensitivity is allowable [15].

The readout of the useful signal using the inner electrostatic system eliminates the need to use radio frequency generators to simplify circuitry and reduces, in GIS, various internal noise that are generated in the sensor [20], hence facilitating a solution to the second problem mentioned previously.

A distinctive feature of the sensor is that the differential electrostatic system performs direct conversion of PM's angular velocity in current flowing in the electrical circuit. The output current of this device is considered as the desired signal.

Dependency of the PM suspension rigidity on the electrostatic field and the presence of alternating electrostatic fields in the sensor allow periodic modulation of the stiffness of the suspension, and as consequence, allow significant parametric amplification of the output current in this sensor. The current's carrier frequency can be set arbitrarily, that allows shifting it to the frequency range with low noise. This feature can solve the third problem described previously.

Parametric transformation and amplification of signals commonly used in designing tiny sensors NEMS and MEMS, started approximately in 1991 [21]. Practically unlimited number of publications are devoted to the study of the properties of systems with parametric excitation. It has been found that such systems have unique features as compared with the systems of external excitation [24, 25]. In particular, in such systems, parametric resonance may occur in several frequency bands (resonance regions), and in the case of linear systems, the maximum value of the oscillation amplitude is not limited in these bands, even if there is energy dissipation. Only the nonlinearity of the parametric system limits the maximum amplitude of the parametric resonance [26]. The dissipation of energy determines the threshold pump amplitude (amplitude modulation), which is a characteristic for each of the resonance zones.

It was proved that the sensors with parametric excitation might have high sensitivity as in a vacuum and in the air [27–30], and sensors with parametric amplification of signals can be more sustainable, cheap and portable [31] compared to sensors with conventional external excitation.

A simple system was first described in [22], in which the parametric amplification of the signal by modulating the torsion rigidity of the mechanical oscillator, in an electric field was observed. The amplifier of this type is of particular interest because it has been proven that the noise in parametric amplifiers can be reduced to a quantum-mechanical level [21]. These results, in principle, can be produced in any structures size [22].

The above-described properties of the parametrically excited systems are promising for use in GIS to achieve high gain and low noise level. However, the results presented in [21] were obtained near the resonance frequency of the parametric pump that is twice the frequency of the resonator. The GG on a movable base have to have a flat frequency response in the range of operating frequency of the order of 1 Hz or less. Therefore, resonance measurement modes should be avoided in the GIS.

On the other side, parametric amplification of the signals in the non-resonant modes at low-frequency range does not usually investigated. However, as far as it is known, Den Hartog was the first who point out that the work of the parametric pump source can be positive, even in the case of a constant external signal, acting on a parametric system [32]. Hence, it issues from this, that the low frequency signals

might be amplified in parametric sensor. We use this feature of parametric system in the sensor is being designed now.

Physical and mathematical models of graviinertial sensor

Figure 1 shows the design scheme of the universal sensor, in which the PM has the form of elastically suspended conductive plate 1. Elastic connection sensor's housing with the PM is presented in the form of a torsion 2, whose axis is perpendicular to the plane of the figure. Two conductive electrodes 4 which are attached with fixed non-conductive plate 3. The electrodes 4 form together with PM two capacitors whose capacitance changes when PM tilts. Capacitors, conductive elements and the PM form an electrical circuit, which includes the sources of direct and alternating voltage. Moreover, for completeness, to be able to investigate in the sensor the influence of penetrating noises, noise sources in the form of discrete noise generators are incorporated in the sensor circuit.

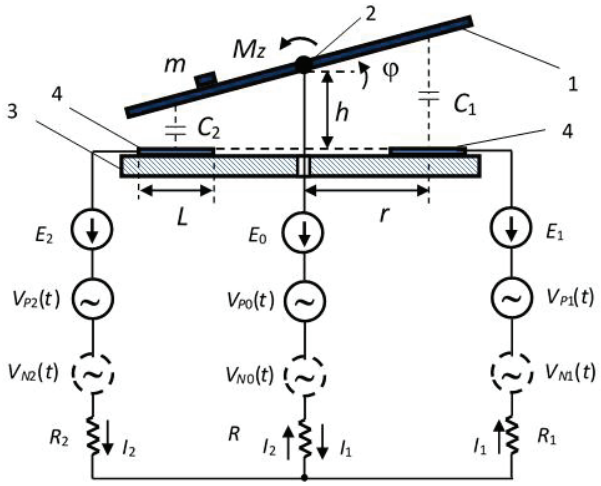

Figure 1 – Universal model of a graviinertial sensor. 1 – conductive proof mass; 2 – elastic torsion; 3 – nonconductive plate; 4 – conductive electrodes; E_0, E_1, E_2 – direct current power supply sources; $V_{p0}(t)$, $V_{p1}(t)$, $V_{p2}(t)$ – deterministic variable voltage sources; $V_{N0}(t)$, $V_{N1}(t)$, $V_{N2}(t)$ – random noise sources; m – a point mass, showing the position of the PM center mass if the sensor is a linear accelerometer

References [33, 34] examined the conditions of static and dynamic stability and modes of free and forced PM vibrations of a similar sensor in the absence of AC sources. It has been shown that the sensor's stability greatly depends on the symmetry of the electrostatic system (ES).

In particular, it was found that significant reduction of stiffness torsion suspension under the action of electrostatic forces, in order to increase the sensitivity of the sensor, it is only possible if the symmetry satisfies stringent requirements of ES. For example, the resonant frequency of the sensor can be reduced tenfold asymmetry if ES does not exceed a few tenths of a percent.

Capacitors, shown in Figure 1, depend on the angle of inclination φ PM. In [33] proposed a method to calculate the capacitors with inclined planes obtained with simple formulas which are convenient for calculating the moments of the forces of the electric field acting on the PM that does not require expansions in powers of the small argument. Using this formula, and assuming that the EC is not symmetrical, introducing electrical asymmetry coefficient γ of this sensor, we have:

$$C_1(x)=\frac{C_s}{1+x},\quad C_2(x)=\frac{(1+\gamma)C_s}{1-x}=\frac{\gamma_1 C_s}{1-x}, \tag{1}$$

where:

$$C_s=\frac{\varepsilon_0 S}{h}, \tag{2}$$

$$\gamma_1=1+\gamma,\ S=L^2,\ x=\varphi/\varphi_m,$$
$$\varphi_m=\frac{h}{L}In\frac{c_2}{c_1},\ c_1=r-\frac{L}{2},\ c_2=r+\frac{L}{2}. \tag{3}$$

If q_1 and q_2 are charges, respectively, in the capacitors C_1 and C_2, the moments of the forces acting on the PM from these charges are given by:

$$M_1=\frac{1}{2}\frac{q_1^2}{C_s\varphi_m},\quad M_2=\frac{1}{2}\frac{q_2^2}{\gamma_1 C_s\varphi_m}. \tag{4}$$

Given the moment of the elastic forces of the suspension and the directions moments of the mechanical and electrical forces, the resulting moment acting on the PM is:

$$M_\varphi=k\varphi-\frac{1}{2}\frac{q_2^2-\gamma_1 q_1^2}{\gamma_1 C_s\varphi_m}. \tag{5}$$

Let, on the PM acts external moment $M(t) = M_z\cos(n\Omega t)$, where Ω is the natural frequency of the sensor in the presence only of a source of constant electric field, n is an arbitrary fixed number; M_z is the amplitude of this moment. Voltages sources of alternating electric field, represented in Figure 1, can be written in the form (i = 0; 1; 2):

$$V_{Pi}(t) = V_i \cos\left(n_1 \Omega_p t + v\frac{\pi}{2}\right);\ V_{Ni}(t) = N_i(t)\cos\left[f_i(t)\right], \quad (6)$$

where V_i – amplitude, Ω_p – the resonant frequency of the sensor in the presence of sources of direct and alternating field; n_1 – arbitrary constant number; v – arbitrary number that allows to set the phase of the parametric pumping relative to the phase of the moment of external force; $N_i(t)$ и $f_i(t)$ – asked random functions to simulate noise on the sensor input. In the calculations we can assume that $V_{Ni}(t) = N_i \cdot rnd(1) \cdot \cos\left\{n_2 \Omega t + 2\pi \sin\left[rnd(1)\right]\right\}$, where $rnd(1)$ – the random number generator, uniformly distributed between zero and one, n_2 – arbitrary number.

Let us introduce further notation:

$$b_1(t) = C_s(E_0 - E_1) + C_s(V_0(t) - V_1(t)) + C_s(V_{N0}(t) - V_{N1}(t)),$$

$$b_2(t) = C_s(E_0 - E_2) + C_s(V_{P0}(t) - V_{P2}(t)) + C_s(V_{N0}(t) - V_{N2}(t)). \quad (8)$$

Applying the laws of Kirchhoff to the circuit in Figure 1 and using the formula (1)–(5), we obtain a system of equations describing the dynamics of the GIS:

$$I_z \ddot{x} + D\dot{x} + kx - \frac{q_2^2 - \gamma_1 q_1^2}{2\gamma_1 C_s \varphi_m^2} = \frac{M_z}{\varphi_m}\cos(n\Omega t), \quad (9)$$

$$I_1 = \frac{dq_1}{dt} = -\frac{\frac{q_2}{\gamma_1} R(1-x) + q_1(R+R_2)(1+x) + Rb_2(t) - (R+R_2)\,b_1(t)}{C_s(RR_1 + RR_2 + R_1 R_2)}, \quad (10)$$

$$I_2 = \frac{dq_2}{dt} = -\frac{q_1 R(1+x) + \frac{q_2}{\gamma_1}(R+R_1)(1-x) + (R+R_1)\,b_2(t) - Rb_1(t)}{C_s(RR_1 + RR_2 + R_1 R_2)}, \quad (11)$$

where I_z – the moment of inertia of the PM with respect to the torsion axis; I_1 and I_2 – currents, as shown in Figure 1. The mathematical model of the sensor, the system described by (9)–(11) is a parametric nonlinear system of differential equations. Exact analytical solutions of the model in general are hardly possible. Therefore, to avoid the «fight against Mathieu equation or Floquet theory» [25], this system will be linearized in order to hold a preliminary analysis and get some interesting relationships between the sensor parameters, and after that the original nonlinear system will be solved numerically. Given that the charges q_1 and q_2 contain constants (q_s) and variable (q_v) components, these charges may be written in the form of:

$$q_1 = q_{1s} + q_{1v}, \quad q_2 = q_{2s} + q_{2v}. \quad (12)$$

If the notations $\tau_1 = C_s(R+R_1)$, $\tau_2 = C_s(R+R_2)$, $\tau = C_s R$ are introduced and then one can be assumed that all the resistors have fairly small values, so that the parameters τ_1, τ_2 and τ considered as small. Also it can be assumed that $q_v << q_s$. Additionally, one can neglect terms containing q_v with degrees higher than the first, as well as members with the time derivative of $b_1(t)$ and $b_2(t)$, containing as a multiplier settings τ_1, τ_2 and τ. Also, a neglect of terms containing the parameters τ_1, τ_2 and τ to a degree higher than the first, and their products may be done.

Below, it is shown that in the case when in parameters $b_1(t)$ and $b_2(t)$ are taken into account only the deterministic voltages sources, in the sensor has to be realized conditions under which the next equality is fulfilled:

$$b_2(t) = \frac{b_1(t)}{\sqrt{\gamma_1}}. \quad (13)$$

For simplicity, the symbol «t» in $b_1(t)$ and $b_2(t)$ sometimes will be omit. Farther, from (13), in particular, it follows the equalities $\frac{1}{b_1}\frac{db_1}{dt} = \frac{1}{b_2}\frac{db_2}{dt}$ and $\frac{1}{b_1}\frac{d^2b_1}{dt^2} = \frac{1}{b_2}\frac{d^2b_2}{dt^2}$, given that one can get for charges q_{1v} and q_{2v} corresponding linear differential equations. Briefly, we write these equations in matrix form:

$$\left[B_4\frac{d^4}{dt^4} + B_3(t)\frac{d^3}{dt^3} + B_2(t)\frac{d^2}{dt^2} + B_1(t)\frac{d}{dt} + B_0(t)\right]\begin{Bmatrix} q_{1v} \\ q_{2v} \end{Bmatrix} = -\begin{Bmatrix} b_1 \\ b_2 \cdot \gamma_1 \end{Bmatrix}\left[\frac{M_z}{\varphi_m}\cos(n\Omega t) + \frac{b_2^2\gamma_1 - b_1^2}{2C_s\varphi_m^2}\right], \quad (14)$$

where, if the notations $\alpha_1 = \tau_1 + \tau_2\gamma_1$, $\alpha_2 = \tau_1\tau_2 - \tau^2$, $D_b = D - 2I_z\frac{1}{b_1}\frac{db_1}{dt}$ are used:

$$B_4 = a_2\gamma_1 I_z;\ B_3(t) = a_1 I_z + a_2\gamma_1 D_b;\ B_2(t) = I_z + a_1 D_b; \quad (15)$$

$$B_1(t) = D_b + a_1\left[k - D_b\frac{1}{b_1}\frac{db_1}{dt} - I_z\frac{1}{b_1}\frac{d^2b_1}{dt^2}\right]; \quad (16)$$

$$B_0(t) = k - \frac{b_1^2 + b_2^2\gamma_1}{C_s\varphi_m^2} - \left[D_b \frac{1}{b_1}\frac{db_1}{dt} + I_z \frac{1}{b_1}\frac{d^2b_1}{dt^2} \right]. \quad (17)$$

Parameters $b_1(t)$ and $b_2(t)$ are defined by formulas (7) and (8). They are independent from moment M_z. Therefore, the second term in square brackets in the right-hand side of equation (14) can be regarded as equivalent to external disturbances acting on the PM. These disturbances are due to the presence of direct current (DC) and AC voltage sources in the sensor's electrical system, as well as the presence of noise in the system. Assuming that the amplitude of the direct and alternating voltage sources can be adjusted, easy to see that the effect of the deterministic part of these external forces can be eliminated by ensuring the condition (13). However, in the case of random uncorrelated signals such regulation is hardly possible, and the random component of the disturbances on the sensor input remains.

One equation can be obtained from two equations in (14) for the sum charges q_{1v} and q_{2v}. The coefficients (15)−(17) in the equations (14) have identical form for both charges q_{1v} and q_{2v}. However, the right-hand sides of equations in (14) differs in view of the factors that are in braces. Taking into account the relation (13), under the total charge will be understood charge q_v, defined by the equation:

$$q_v = \sqrt{\gamma_1} q_{1v} + q_{2v}. \quad (19)$$

Then, when the conditions (13) and (19) have been satisfied, the desired equation for the total charge q_v takes the form:

$$B_4 \frac{d^4q_v}{dt^4} + B_3(t)\frac{d^3q_v}{dt^3} + B_2(t)\frac{d^2q_v}{dt^2} + B_1(t)\frac{dq_v}{dt} + B_0(t)q_v = -2b_1\sqrt{\gamma_1}\frac{M_z}{\varphi_m}\cos(n\Omega t). \quad (20)$$

Factors B_3 and B_4 are small. If to neglect the corresponding term in the equation (20), this equation can be simplified and written as:

$$B_2(t)\ddot{q}_v + B_1(t)\dot{q}_v + B_0(t)q_v = -2b_1\sqrt{\gamma_1}\frac{M_z}{\varphi_m}\cos(n\Omega t). \quad (21)$$

Given that the current is $I = \frac{dq}{dt} = \frac{dq_v}{dt}$, from expressions (19) for the total current one have:

$$I_{out}(t) \equiv I(t) = \sqrt{\gamma_1} I_1 + I_2. \quad (22)$$

Formulas for calculating the currents I_1 and I_2 are given by (10) and (11). If one have an expression for the total current, it can be seen that the total current contains factors $b_1(t)$ and $b_2(t)$. As already mentioned, the relevant terms are background signals, because they do not contain measured signal amplitude M_z. These background signals can significantly exceed the useful signals. It can be found, that the conditions of suppression of background signals is given by the condition (13).

Let assume, as above, that the voltage sources are deterministic (and can be adjusted). Also, for simplicity, it is assumed that the phases of all sources of noise are correlated with each other, but the values of their amplitudes cannot be adjusted. Then from (10)–(11) it can be found that the deterministic component of the background signal in the total output current (22) will be absent if the following conditions are fulfilled:

$$E_0 - E_1 = \sqrt{\gamma_1}\left(E_0 - E_2\right), \quad (23)$$

$$V_0 - V_1 = \sqrt{\gamma_1}\left(V_0 - V_2\right), \quad (24)$$

$$\gamma_1\left(R + R_2\right) = \left(R + R_1\right). \quad (25)$$

When the conditions (23)–(25) for suppression of the background signal entering the output signal are satisfied, the issues from the formulas (10) and (11) that the output current $I_{out}(t)$ will have the form:

$$I_{out}(t) = -\frac{q_{2v} + q_{1v}\sqrt{\gamma_1} - x\left(q_{2v} - q_{1v}\sqrt{\gamma_1}\right)}{C_s\left(R + R_1 - R\sqrt{\gamma_1}\right)} - \frac{\left(\sqrt{\gamma_1} - 1\right)N_0 - \left(\sqrt{\gamma_1}N_2 - N_1\right)}{\left(R + R_1 - R\sqrt{\gamma_1}\right)} \cdot \sqrt{\gamma_1} \cdot rnd(1) \cdot \cos\left\{n_2\Omega t + 2\pi\sin\left[rnd(1)\right]\right\}. \quad (26)$$

Dependency of $I_{out}(t)$ can be calculated numerically, if to solve a system of (9)–(11) and to find the charges q_{1v} and q_{2v} as functions of time.

From the form of the second term in formula (26) that when the sensor ES asymmetry is small, i.e. $\gamma_1 \approx 1$, the influence of noise generated in the central part of the circuit (Figure 1) that is the proportional amplitude N_0 is significantly attenuated. It also shows that in this case, noises N_1 and N_2 that were generated in the side chain

branches also cancel each other if they are in identical phase.

The elastic coefficient $B_0(t)$ in equation (20), contains a constant and a variable parts (Eq. (17)). Permanent part determines the resonant frequency of the sensor. For simplicity, we assume that additional voltage source are absent, i.e. $E_1 = 0$ V and $V_1 = 0$ V. Then, if there are conditions (23)–(24), the resonant frequency of the sensor will look like Eq. (27):

$$\Omega_p = \sqrt{\omega_0^2 - 2\frac{C_s}{I_z\varphi_m^2}\left(E_0^2 + \frac{1}{2}V_0^2\right)} = \sqrt{\Omega^2 - \frac{C_s}{I_z\varphi_m^2}V_0^2}, \quad (27)$$

where $\omega_0 = 2\pi f_0 = \sqrt{\frac{k}{I_z}}$ – is the resonant frequency of the sensor in the absence of an electric field; and

$$\Omega = \sqrt{\omega_0^2 - 2\frac{C_s}{I_z\varphi_m^2}E_0^2} \quad (28)$$

– the square of the resonant frequency of the sensor in the presence of the constant electric field and in the absence of the alternating electric field.

From formulas (27) and (28) it follows that the resonant frequency of the sensor depends on the stiffness k and on the voltages E_0 and V_0. Such presence of electric fields reduces the torsional rigidity of the PM suspension that allows an increase of the sensitivity of the sensor without reducing the hardness of the suspension.

If AC voltage sources are absent and frequency Ω have been set, from (28) it may be found the value of the voltage E_0 a constant electric field, in which this frequency is achieved:

$$E_0 = \varphi_m\sqrt{\frac{I_z\left(\omega_0^2 - \Omega^2\right)}{2C_s}} = \varphi_m\sqrt{\frac{k - I_z\Omega^2}{2C_s}}. \quad (29)$$

The value of the amplitude of the alternating field voltage V_0 at which the frequency setpoint Ω_P, it follows from formula (27):

$$V_0 = \varphi_m\sqrt{\frac{I_z\left(\Omega^2 - \Omega_p^2\right)}{C_s}} = \varphi_m\sqrt{\frac{1}{C_s}\left(k - 2\frac{C_s}{\varphi_m^2}E_0^2 - I_z\Omega_p^2\right)}. \quad (30)$$

From (30) is seen that for a setpoint Ω, the maximum value $V_0 = V_{0max}$ of an alternating field amplitude at which $\Omega_P = 0$ is:

$$V_{0\max} = \varphi_m\sqrt{\frac{1}{C_s}\left(k - 2\frac{C_s}{\varphi_m^2}E_0^2\right)}. \quad (31)$$

As mentioned above, the sensor circuit shown in Figure 1, can be used to measure the various physical quantities. For this purpose, in each case it is necessary to determine the bond M_z acting on the PM with the measured signal. In particular, if the gradient of the gravitational field, denoted as Γ, is a measured value, this bond is $M_z = I_z$. It should be noted that this formula is too simplified. In reality, the bond of M_z and gradient Γ is more complicated [2, 39, 40]; if the measured value is the angular acceleration «*e*», of a sensor revolving around the torsion axis, the bond is $M_z = I_z\, e$; if the measured value is a component of the linear acceleration of a sensor revolving perpendicular to the axis of the torsion «*a*», the bond is:

$$M_z = mra = mrg\,(a/g), \quad (32)$$

where r – a distance from the center of mass of the PM to the torsion axis; g – is a free fall acceleration.

The new principle in designing the GIS that was stated above including parametric transformation and amplification of the input signal is considered as an example of the micromechanical linear accelerometer. To simplify the numerical analysis, it will be assumed that the sources of constant voltage E_0, E_1 and E_2 are absent. In addition, it will be assumed that an additional source of AC voltage $V_{P1}(t)$ and all sources of noise $V_{N0}(t)$, $V_{N1}(t)$ and $V_{N2}(t)$ are also absent. It is assumed Also that the phase setting $v = 0$ (see Eq. (6)). Under these conditions, a generalized scheme (Figure 1) transforms in the equivalent scheme is shown in Figure 2.

Subject to the above formulas (23)–(25) for compensation of the background current I_b, some other formulas are simplified, and they take the next form of: frequency $\Omega = \omega_0$, the value of the resonant frequency of the sensor Ω_P is calculated by formula (33).

$$\Omega_p = 2\pi f_p = \sqrt{\omega_0^2 - \frac{C_s}{I_z\varphi_m^2}V_0^2} \quad (33)$$

the maximum allowable amplitude of the alternating field is defined as:

$$V_{0\max} = \varphi_m\sqrt{\frac{k}{C_s}} = \varphi_m\omega_0\sqrt{\frac{I_z}{C_s}}. \quad (34)$$

If to assume that the amplitude V_0 has been set, the condition for suppression of the background current I_b (it is the AC voltage source with an amplitude V_2 that is used for this aim) takes the form:

$$V_2 = V_0\sqrt{\gamma_1 - 1} = V_0\sqrt{\gamma}. \quad (35)$$

Layout Options of the micromechanical accelerometer and results of calculations

We assume that the PM is made of technical silicon with the density ρ = 2.4 g / cm^3, and it has a square shape with a side length of L = 12 mm and a thickness of d = 0.36 mm. The horizontal distance from the axis of the torsion to the middle of the electrode r = 6.5 mm; the gap between the electrodes and the PM h = 0.015 mm (see Figure 2).

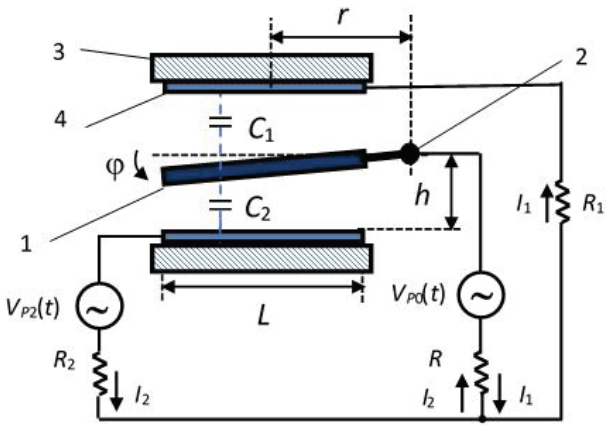

Figure 2 – Scheme of a linear micromechanical accelerometer with parametric conversion and amplification of the signal, similar to the scheme in Figure 1: 1 – moving mass; 2 – elastic torsion; 3 – insulating substrate; 4 – electrode

Conductive electrodes have also a square shape with a side length of more than 12 mm. Also, it is assumed that the natural frequency of the PM in the absence of an electric field was set to f_0 = 30 Hz and the resistance values $R = R_2$ = 5 Ohm. The value of the resistor R_1 is determined by the formula (25), if the value of the coefficient of asymmetry of electrostatic system γ is known.

Calculation of the formulas (3) gives the value of C_s = 84.96 pF, the value of angle $\varphi_m = 4.024 \cdot 10^{-3}$, the mass of PM is given the obvious estimate $m = \rho L^2 d = 1.244 \cdot 10^{-4}$ Kg. PM inertia moment about the axis of rotation (torsion axis) is calculated by the well-known formula:

$$I_z = \frac{1}{12} mL^2 + mr^2, \tag{36}$$

that gives $I_z = 6.75 \cdot 10^{-9}$ Kg·m^2.

The calculation of the remaining sensor parameters begin with the calculation of the allowable maximum value of the AC voltage amplitude by formula (34): V_{0max} = 6.76 V. The value of the viscous damping coefficient D, included in the formulas (9) and (15)–(17), will be calculated from the known relationship D and quality factor Q, as $D = I_z \omega_0 / Q$. In the calculations, two values of the quality factor were used: Q = 1000 and Q = 2.

The above formulas (23)–(25) for compensation of the background current I_b, were obtained from an analysis of the linearized mathematical model of the sensor. Numerical calculations showed that these conditions are well satisfied in the original non-linear model providing suppression of signals from these sources. However, if at least one of these conditions is fulfilled with an error, the background current (i.e. the component of the current I_b in the output of the sensor) will penetrate into the output signal from the AC voltage sources. The said compensation error can be accounted for in the calculations, if for example, formula (35) is rewritten as:

$$V_2 = V_0 (1 + \varepsilon) \sqrt{\gamma}. \tag{37}$$

According to the calculations, to suppress current I_b, the more the parameter of asymmetry γ, the more requirement for permissible error ε. The asymmetry coefficient values that will be used in the calculations is γ = 0.01 and the requirement for error performing conditions compensation is ε = 0.001.

Below are the results of the accelerometer calculations for two values of voltage V_0 satisfying to condition $V_0 < V_{0max}$. These values are: $V_0 \equiv V_{01}$ = 0.1 V and $V_0 \equiv V_{02}$ = 6.7 V. In these cases, as follows from formula (33), the accelerometer design will have the following resonance frequencies $f_{p1} \approx 29.997$ Hz $\approx f_0$ and $f_{p2} \approx 3.988$ Hz, respectively. The calculation of the compensating voltage V_2 is held by the formula (37).

Let define the sensitivity parameter of the sensor as a ratio of output amplitude to the amplitude of the measured acceleration: $S = I_{out}/a$. In Figure 3, the amplitude-frequency characteristics of the accelerometer sensitivity are shown.

The left axis in Figure 3 represents the sensitivity of the sensor as a coefficient that links the output signal as amplitude of the current (22) and output signal as amplitude linear acceleration of a housing:

$$I_{out} = S(nf_0)\, a(nf_0). \tag{38}$$

AC power source frequency was chosen from the next conditions: at V_0 = 0.1 V the dimensionless parameter n_1 = 60, so that the pump frequency $n_1 f_{p2} \approx$ 1800 Hz (see formula (6)). In another embodiment: at V_0 = 6.7 V the parameter n_1 = 451, so that the pump frequency was the same 1800 Hz, i.e.

$n_1 \cdot f_{p1} \approx 1800$ Hz. Another embodiment of the sensor: at the same value $V_0 = 6.7$ V the parameter $n_1 = 60$, so that the pump frequency was $n_1 \cdot f_{p1} \approx 239.3$ Hz. In Figure 3, three solid curves relate to the sensors for which $Q = 1000$ and the three dotted curves relate to sensors for which $Q = 2$.

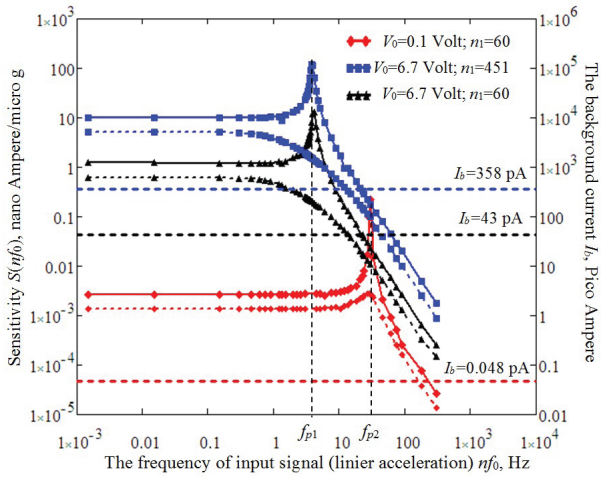

Figure 3 – The amplitude-frequency characteristics of the sensitivity of sensors with different resonance frequencies and the levels of background signals that generated at the output of these sensors by parametric pumping sources, if $\gamma = 0.001$ and $\varepsilon = 0.001$. I_b – background on the current output of the sensor at $M_z = 0$

The right axis in Figure 3 refers to the values of the amplitudes of the components of the background current I_b in the sensor with $Q = 1000$ are got at values $\gamma = 0.001$ and $\varepsilon = 0.001$. These currents are represented by horizontal dashed lines. The lower line relates to the sensor with resonant frequency f_{p2} at $n_1 = 60$; the average line refers to sensor with resonant frequency fp_1 at $n_1 = 60$; the upper line relates to the sensor with resonant frequency f_{p1} at $n_1 = 451$. By reducing the Q value of the sensor to $Q = 2$, the values of the currents I_b, provided by the upper and middle straight lines are halved, and the value of the current is represented by a straight bottom line does not change.

In these sensors at $M_z = 0$ and $\gamma = 0$, or $\varepsilon = 0$, the background current $I_b = 0$. This proves that in the symmetric sensor, or, in the sensor, which accurately satisfies the conditions of compensation (23)–(25), it is indeed the background signal that does not penetrate into the output signal. The current value I_b, generated when $\varepsilon \neq 0$, restricts the minimum value of acceleration that can be measured by the sensor. This value may be determined by solving the non-linear system (9)–(11) and (22) when adjusting the value of the acceleration a, which define the equality $I_{out} = I_b$. In these circumstances, the value of $I_{out} = 0.048$ pA in the sensor with voltage $V_0 = 0.1$ V and with the pump frequency of $60 \cdot f_{p2} \approx 1800$ Hz meets the acceleration with the value $a = a_{min1} \approx 1{,}5 \cdot 10^{-7}$ g. In sensors with a voltage $V_0 = 6.7$ V and with the pump frequency of $451 \cdot f_{p1} \approx 1800$ Hz, and with the pump frequency of $60 \cdot f_{p1} \approx 39.3$ Hz, the current values I_b, respectively, equal to 358 pA and 43 pA were obtained approximately at the same values minimum acceleration $a = a_{min2} \approx 3 \cdot 10^{-7}$ g.

The maximum accelerations amax, measured by the sensor, determines the value of the acceleration a, for which the system of equations (9)–(11) did not have a solution. It was found that in the sensor with a pump frequency of $60 \cdot f_{p2} \approx 1800$ Hz the acceleration $a = a_{max1} \approx 0.58$ g. In the sensor with a pump frequency $451 \cdot f_{p1} \approx 1800$ Hz the acceleration $a = a_{max2} \approx 5.4 \cdot 10^{-4}$ g and in the sensor with a pump frequency $451 \cdot f_{p1} \approx 239$ Hz the acceleration $a = a_{max3} \approx 6.35 \cdot 10^{-4}$ g. It may to be noted that in the sensors, the nonlinear distortion of the dependence I_{out} on a appears when $a \approx 0.1 a_{max}$.

Figure 4 shows the dependence of the accelerometer output signal at $Q = 1000$ on the input signal in all ranges of valid input signal values (symbols in this graph correspond to those in Figure 3). From this, it can be clearly seen that the sensor with the maximum resonant frequency has a maximum dynamic range where the sensitivity of the sensor has linear dependence on the input signal, up to $a/g = 0.1$.

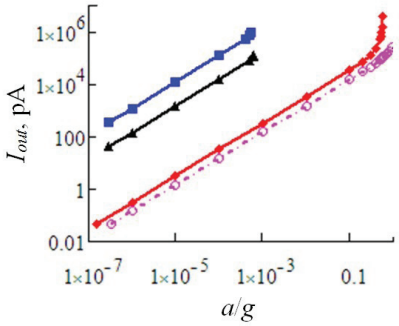

Figure 4 – Dependence of the accelerometer output signal on the input signal. Symbols in the three upper graphs agree to those in Figure 3. The lowest graph corresponds to the process on Figure 6

The available current I_b in the sensor output indicates the presence of asymmetry of electrical circuit. This current can be used to reduce the error ε compensation of asymmetry by manual or automatic control voltage V_2 and the resistance R_2 to eliminate this current (see formulas (25) and (37)). In this case, the dynamic range of the accelerometer measurements can be extended towards small values of the measured signals.

Figures 5*a–e* shows the dependence of the output signal, expressed in pico Ampere, on time, expressed in seconds, for a sensor having a pump voltage $V_0 = 0.1$ Volt, the quality factor $Q = 1000$ and the pumping frequency of 1800 Hz, during measurement of linear acceleration with the amplitude $a = 5 \cdot 10^{-3} g$ that harmonically varying with different frequencies: (*a*) is the DC signal; (*b*, *d*) are the signals with the frequency of 1 Hz and (*c*) is the signal with the resonance frequency $f_{p2} \approx 29.9967$ Hz. Figure 5*e* shows the dependence on the action of a constant acceleration having the maximum amplitude $a_{max1} = 0.58\ g$. Comparing this figure with Figure 5*a* allows to see the effect of non-linear distortion in the output signal of the accelerometer.

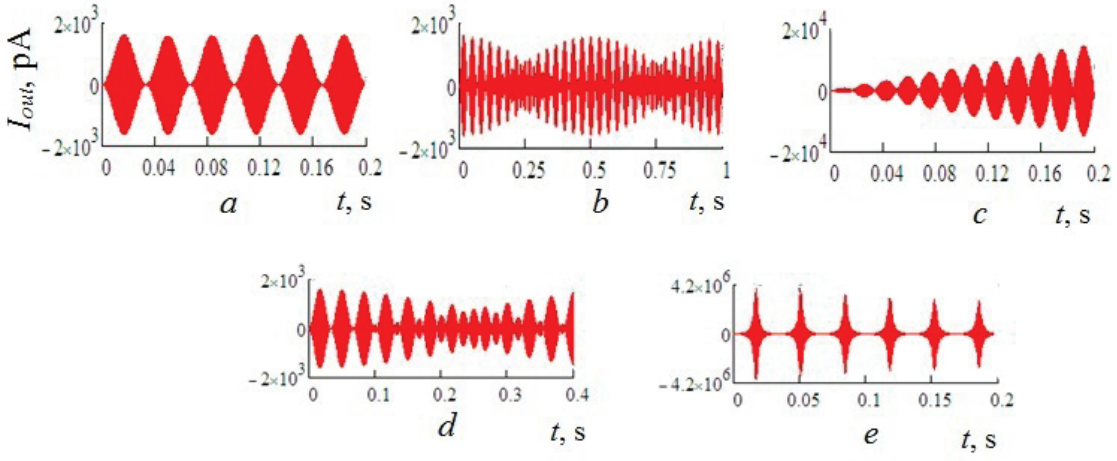

Figure 5 – The dependence on times of the accelerometer output signal with the parameters of $f_0 = 30$ Hz, $V_0 = 0.1$ Volt, $f_{p2} \approx 29.997$ Hz and $n_1 = 60$ for different values of the input signal frequency nf_0: $a - n = 0$; b, $d - nf_0 = 1$ Hz; $c - nf_0 = f_{p2}$ (resonance); $e - n = 0$, $a = a_{max1} = 0.58\ g$

The forms dependencies in Figures 5 are determined by the period of the beat $T_b = 1/|f_{p2} - nf_0|$ resulting by adding the signal with a frequency equal to the frequency $n \cdot f_0$ of the measured signal and the signal with the frequency, f_{p2} is equal to the natural frequency of the sensor.

In the sensor with parametric pumping, it is possible to extend the dynamic range of the sensor to higher values of the measured signal. This possibility is illustrated in Figure 6, where *a* presents the output signal of the accelerometer in the case when the sensor has voltage $V_0 = 0.1$ V and $Q = 1\ 000$ leading to a constant acceleration $a = 0.60$ g, which is greater than the maximum allowable acceleration $a_{max1} = 0.58$ g. It can be seen, that the sensor is in an unstable mode, since the output current increases unlimitedly with time.

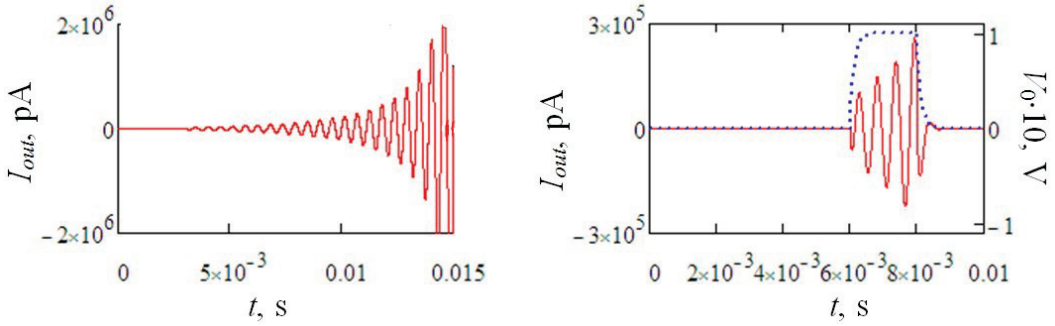

Figure 6 – The method for measuring by the sensor that is in unstable mode. *a* – proof mass oscillations in unstable mode at $a = 0.6$ g$> a_{max}$. *b* – proof mass oscillation in unstable mode when $a \approx 0.9$ g, but the voltage $V_{P0}(t)$ (dotted curve) is switched on for a short time

Figure 6, *b* shows that, if the sensor with former V_0 and Q is activated only for a certain period of time (in this case, by 0.002 seconds), unlimited current growth is absent, even when the measured acceleration $a = 0.9$ g $> a_{max1}$. The dependence of the output current over the entire range of changes of

acceleration $a_{min} = 1.5 \cdot 10^{-7} g < a < a_{max} = 0.9$ g for this case is represented by the dashed line in Figure 4. It is seen, that Iout has linear relationship that is wider than in previous occasions. It is obvious that such pulsed switching voltage $V_{P0}(t)$ (see formula (6)) can be repeated any number of times during the one cycle measurements.

The parameters of the micromechanical accelerometer that have been used in the calculations are only to illustrate new possibilities. They are not optimized for a particular measurement task, and can be varied considerably.

Conclusion

In the non-linear sensor with parametric transformation of the measured signal where there are many unique features, the design study requires special consideration. The above calculations in its simplest form have shown that some of these features allow implementing fundamentally new graviinertial sensor scheme and new measurement modes, securing great sensitivity.

This sensor has the new features as follows. The alternating electric field allows fulfilling the direct conversion of the angular speed of the proof mass in the alternating current in the sensor. In addition, the electric field allows to reduce and modulate the elasticity of the hanger and to carry out parametric amplification of the output electric current, even if the constant input signal is measured.

Notable features of parametric amplification of signals found in the literature, gave reasons to assume that the developed design GIS has the lowest achievable level of thermal and excess noise generated in the sensor.

Asymmetry of the electrostatic system in the sensor limits its sensitivity and causes the appearance in the output signal with alternating current generated by an alternating voltage source. The use of an additional source of alternating electric field allows to compensate this asymmetry and to reduce the background current. More compensation can be done by balancing resistance electrical circuits in the sensor. The relations between amplitudes of voltage sources and the values of resistors from one side with values of the asymmetry factor γ and with permissible error of compensation and of balancing ε, from other side, when the background current is absent, have been given. The requirement for error ε compensation and balancing increases with increasing coefficient of asymmetry γ.

As an example, numerical calculations of the micromechanical linear accelerometer were carried out. In particular, it has shown that if the parameters γ and ε do not exceed 0.1 %, a sensor with a resonant frequency of about 30 Hz, using an alternating voltage with an amplitude of 0.1 Volts and pumping frequency at 1800 Hz has a sensitivity that depends almost linearly on the acceleration amplitude in the range of $1.5 \cdot 10^{-7}$ g < a < 0.1 g. The calculated frequency response of the sensor is a horizontal in frequency range below 10 Hz, where the output signal amplitude is equal to approximately 7.3 nano Ampere. With increasing the voltage of the pump generator, sensor's sensitivity is increased, however, dynamic range and linearity range are reduced.

It should be noted that the calculations of the dynamics of a micromechanical sensor were carried out in the transition mode, moving mass oscillation that does not really matter for a relative small time of measurement. Besides, it was shown the possibility of the existence of the acceleration measurement method in an unstable oscillation mode proof mass, with the proviso that the envelope of the pumping voltage is a pulse with a duration greater than the duration of several periods of the pumping.

Graviinertial sensor design theory is universal; it is applicable to any pendulum sensor with a differential capacitive system. The next challenge will be to build the sensor and test its sensitivity despite possible manufacturing issues.

References

1. Gilavdary I., Riznookaya N. Stages of development and state of engineering of gravity gradiometers for moving objects (Review). *Devices and Methods of Measurements*, 2016, vol. 7, no. 3, pp. 122–128 (in Russian). **doi:** 10.21122/2220-9506-2016-7-3-235-246

2. Annecchione M., Moody M., Carroll K., Dickson D., Main B. Benefits of a high performance airborne gravity gradiometer for resource exploration. *Fifth Decennial International Conference on Mineral Exploration*, 2007, pp. 889–893.

3. Konecny G. Small satellites – A tool for Earth observation? *XXth ISPRS Congress-Commission*, 2004, vol. 4. Available at: http://www.cartesia.org/geodoc/isprs2004/comm4/papers/428.pdf (accessed 27.02.2017).

4. Carroll K. Gravity gradiometry for lunar surface exploration. *42nd Lunar and Planetary Science Conference*, 2011. Available at: https://www.researchgate.net/profile/Kieran_Carroll/publication/264340952_Gravity_Gradiometry_for_Lunar_Surface_Exploration/links/53d910cb0cf2631430c3a510/Gravity-Gradiometry-for-Lunar-Surface-Exploration.pdf (accessed 27.01.2017).

5. Stibrany P., Carroll K.A. The microsat way in Canada. *Proc. 11th CASI Conference on Astronautics*, 2001. Available at: http://citeseerx.ist.psu.edu/viewdoc/download?doi=10.1.1.199.676&rep=rep1&type=pdf (accessed 27.02.2017).

6. Carroll K.A., Spencer H., Zee R.E. An Asteroid Lander/Rover for Asteroid Surface Gravity Surveying. *Small Satellite Conference*, 2016. Available at: http://digitalcommons.usu.edu/cgi/viewcontent.cgi?article=3408&context=smallsa (accessed 10.03.2017).

7. Spencer H. Lunette: Lunar Farside Gravity Mapping by Nanosat. *19th Annual AIAA/USU Conference on Small Satellites*, 2005. Available at: http://digitalcommons.usu.edu/cgi/viewcontent.cgi?article=1635&context=smallsat (accessed 19.10.2016).

8. Evstifeev M.I. The state of the art in the development of onboard gravity gradiometers. *Gyroscopy and Navigation*, 2017, vol. 8, no. 1, pp. 68–79.
doi: 10.1134/S2075108717010047

9. Ghose K., Dandavino S., Meyer H., Chamot B. and j.-f. labrecque-piedboeuf et al. Gravity gradient earth sensor experiment on rexus 11. *21st ESA Symposium on European Rocket and Balloon Programmes*, Thun, Switzerland, June 9–13, 2013. Available at: https://infoscience.epfl.ch/record/187717/files/ghose%20ESA%20Thun%202013.pdf (accessed 12.11.2016).

10. Allen J. Micro-System Inertial Sensing Technology Overview. Albuquerque, New Mexico, 2009, 32 p.

11. Tutorial: Noise in micromechanical systems. MEMS material. Available at: http://www.kaajakari.net/~ville/research/tutorials/tutorials.shtml (accessed 19.10.2016).

12. Li J., Fang J., Du M., Dong H. Analysis and fabrication of a novel MEMS pendulum angular accelerometer with electrostatic actuator feedback. *Microsystem technologies*, 2013, vol. 19, no. 1, pp. 9–16.

13. Yazdi N., Ayazi F., Najafi K. Micromachined inertial sensors. *Proceedings of the IEEE*, 1998, vol. 86, no. 8, pp. 1640–1659.

14. Vasilescu G. Electronic noise and interfering signals: principles and applications. Springer Science & Business Media, 2006, 709 p.

15. Cuperus R. MEMS based gravity gradiometer for Space Application. Available at: https://escies.org/download/webDocumentFile?id=7188 (accessed 19.10.2016).

16. Jiang X., Wang F., Kraft M., Boser B.E. An integrated surface micromachined capacitive lateral accelerometer with 2μG/Ц Braginskii V.B., Manukin, A.B. Measurement of weak forces in physics experiments. Chicago, University of Chicago Press, 1977, 161 p.

17. Ghose K. MEMS Inertial Sensor to Measure the Gravity Gradient Torque in Orbit. *Pour l'obtention du grade de docteur ès sciences école polytechnique fédérale de Lausanne*, 2012, no. 5231. Available at: http://infoscience.epfl.ch/record/169608/files/EPFL_TH5231.pdf (accessed 19.10.2016).

18. Flokstra J., Cuperus R., Wiegerink R.J., van Essen M.C. MEMS based gravity gradiometer for future planetary missions. *Cryogenics*, 2009, vol. 49, iss. 11, pp. 665–668. **doi**: org/10.1016/j.cryogenics.2008.12.019

19. Vasilescu G. Electronic Noise and Interfering Signals. Principles and Applications. *Springer*, 2005, 715 p.

20. Rugar D., Grutter P. Mechanical Parametric Amplification and Thermomechanical Noise Squeezing. *Physical Review Letters*, 1991, vol. 67, no. 6, pp. 699–702.

21. Carr D.W., Evoy S., Sekaric L., Craighead H.G., Parpia J.M. Parametric amplification in a torsional microresonator. *Applied Physics Letters*, 2000, vol. 77, no. 10, pp. 1545–1547.

22. Rescia S. Precise Measurements of Small Linea and Angular Displacements with Capacitance Methods. *Brookhaven National Laboratory.* Available at: http://www.bnl.gov/edm/papers/Sergio_Rescia_020118.pdf (accessed 19.02.2017).

23. Zhang W., Turner K. Noise analysis in parametric resonance based mass sensing. *Proceedings of IMECE04 2004 ASME International Mechanical Engineering Congress and Exposition*. Anaheim, 2004, 5 p.

24. Butikov E.I. Parametric excitation of a linear oscillator. *European Journal of Physics*, 2004, vol. 25, no. 4, pp. 535–554.

25. Schmidt G. *Parametererregte Schwingungen*. Berlin; VEB Deutscher Verlag der Wissenschaften, 1975, 313 p. (publishing European journal of physics. Eur. J. Phys, 2004, vol. 25, pp. 535–554.)

26. Zhang W., Turner K. Application of parametric resonance amplification silicon micro-oscillator based mass sensor. *Sensors and Actuators A: Physical*, 2005, vol. 122, no. 1, pp. 23–30.

27. Yang Y.T., Callegari C., Feng X.L., Ekinci K.L., Roukes M.L. Zeptogram-Scale Nanomechanical Mass Sensing. *Nano Letters*, 2006, vol. 6, no. 4, pp. 583–586.

28. Yang Y.T. Phase noise of nanoelectromechanical systems. Pasadena, California Institute of Technology, 2004, 157 p.

29. Cleland A.N. Thermomechanical noise limits on parametric sensing with nanomechanical resonators. *New Journal of Physics*, 2005, vol. 7, no. 1, p. 235.

30. Yie Z., Zielke M.A., Burgner C.B., Turner K.L. Comparison of parametric and linear mass detection in the presence of detection noise. *Journal of Micromechanics and Microengineering*, 2011, vol. 21, no. 2, pp. 025027.

31. Den Hartog J.P. Mechanical Vibrations. New York, dc McGraw-Hill Book Company, 1956, 464 p.

32. Gilavdary I., Mekid S., Riznookaya N. [Controlling sensitivity of the sensor with differential electrostatic transducers]. *Pribory i metody izmerenii* [Devices and Methods of Measurements]. 2015, vol. 6, no. 2, pp. 163−172 (in Russian).

33. Gilavdary I., Mekid S., Riznookaya N., Abdul Sater A. Static and dynamic stability of gravi-inertial sensors with capacitive differential system of sensitivity adjustment. *Pribory i metody izmerenii* [Devices and Methods of Measurements]. 2016, Vol. 7, no. 1, pp. 16 – 23. **doi:** 10.21122/2220-9506-2016-7-1-16-23

38. Changhoug Guan. Development of a Closed-loop MEMS Capacitive Force Sensor. A Thesis of Master of Science for the Degree Mechanical Engineering. Raleigh. North Carolina, 2009, 90 p.

39. Christophe B., Marque J-P., Foulon B. Accelerometers for the ESA GOCE mission: one year of in-orbit results. *GPHYS SYMPOSIUM,* Paris, 2010, 26 p.

40. Silvestrin P. Control and navigation aspects of the new Earth observation missions of the European Space. *Annual Reviews in Control*, 2005, vol. 29, no. 2, pp. 247–260.

41. Steiger C., Romanazzo M., Emanuelli P.P., Floberghagen R., Fehringer M. The Deorbiting of ESA's Gravity Mission GOCE–Spacecraft Operations in Extreme Drag Conditions. Proceedings SpaceOps, Pasadena, USA, 2014, 12 p.

42. Miller A.H. The theory and operation of the Eotvos torsion balance. *The Journal of the Royal Astronomical Society of Canada*, vol. 28, no. 1, January, 1934, 34 p.

43. Metzger E.H., Jirdtano A., Affleck C. Satellite borne gravity gradiometer study. Buffalo, NASA Goddard space flight center, 1976, 62 p.